

INAF-Osservatorio astronomico di Torino

Technical Report nr. 152

LCTF Wavefront error characterization

G. Capobianco¹, S. Vives², E. Hugot²

¹ INAF- Osservatorio Astronomico di Torino

² Laboratoire d'Astrophysique de Marseille

Pino Torinese, 25th july 2011



LCTF Wavefront error characterization



Index

Index	2
Index of Figures	2
List of Acronyms	2
Revision Log	2
Introduction	3
Set-up	4
Data Acquisition Procedure	5
Data Analysis	6
Conclusions	8

Index of Figures

Figure 1 – Mechanical assembly of the LCTF. From left: the pre-filter, the LCPR and the multistage LC Lyot filter	3
Figure 2 – Schematic view of the set-up	4
Figure 3 – Picture of the set-up	4
Figure 4 – Interferogram [OPD] of the LCTF	5
Figure 5 – Variations of the 2 nd order Zernike parameters	7
Figure 6 – Imaging quality normalized to the set-up aberrations	7

List of Acronyms

LCPR	Liquid Crystals Polarization Rotator
LCTF	Liquid Crystals Tunable Filter
OPD	Optical Path Difference
WFE	Wavefront Error

Revision Log

<i>Date</i>	<i>Issue</i>	<i>Release</i>	<i>Released by</i>	<i>Comment</i>
2011.05.25	0	0	G.Capobianco	First issue
2011.06.06	0	1	S.Vives	Document revision
2011.07.25	0	1	G. Capobianco	Document formatted for OATo TR

Introduction

The purpose of this test is to characterize the WFE of the LCFP and measure its evolution in function of the voltage applied to the LCFP (i.e. when the LCFP scans in wavelength). The LCFP has been designed for the ASIICS\PROBA-3 mission: its properties are summarized in Table 1, and the mechanical assembly is shown in Figure 1.

Measurements have been performed at LAM.

LCTF General	Length [mm]	90
	Diameter [mm]	60
	Aperture [mm]	20
	Number of stages	4
	FSR [nm]	2,7
	FWHM [nm]	0,15
	Center wavelength [nm]	528,64 - 533,38
	Tuning step [nm]	0,01
Pre-filter	Manufacturer	Andover Corp.
	Center wavelength [nm]	530,69
	FWHM [nm]	1,89
LCPR	Manufacturer	MLO
	Rotation angles [deg]	0 - 180

Table 1 – LCTF properties

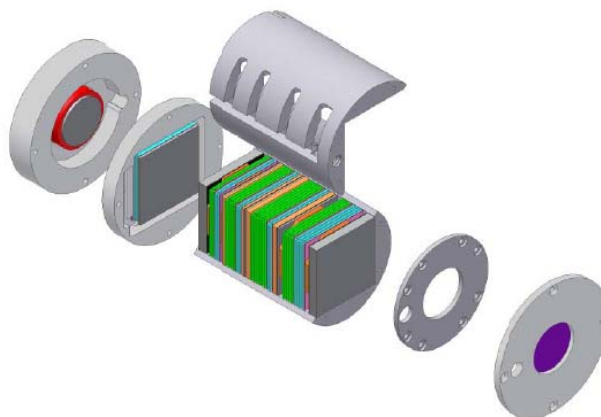


Figure 1 – Mechanical assembly of the LCTF. From left: the pre-filter, the LCPR and the multistage LC Lyot filter

Set-up

The LCFP has been tested in a double pass configuration. The set-up (Figure 2 and Figure 3) was composed by the ADE Phase Shift MiniFIZ a Fizeau interferometer with a reference flat mirror. In order to perform these measurements the pre-filter and the LCPR have been removed from the LCTF. Note that during the measurement, the LCFP was not controlled in temperature.

The objective lens is used as reducer to fit the clear aperture of the LCFP.

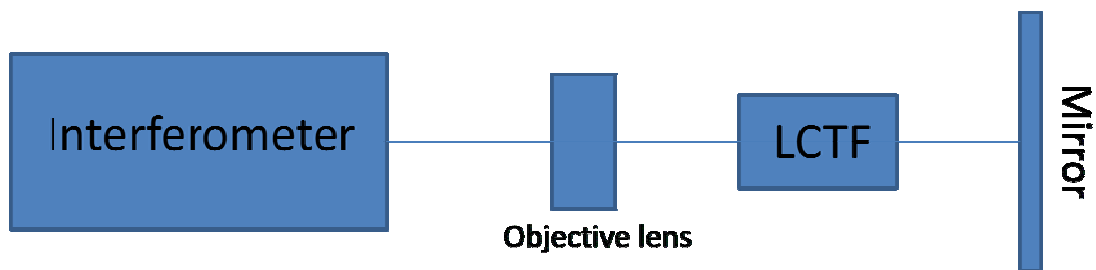


Figure 2 – Schematic view of the set-up

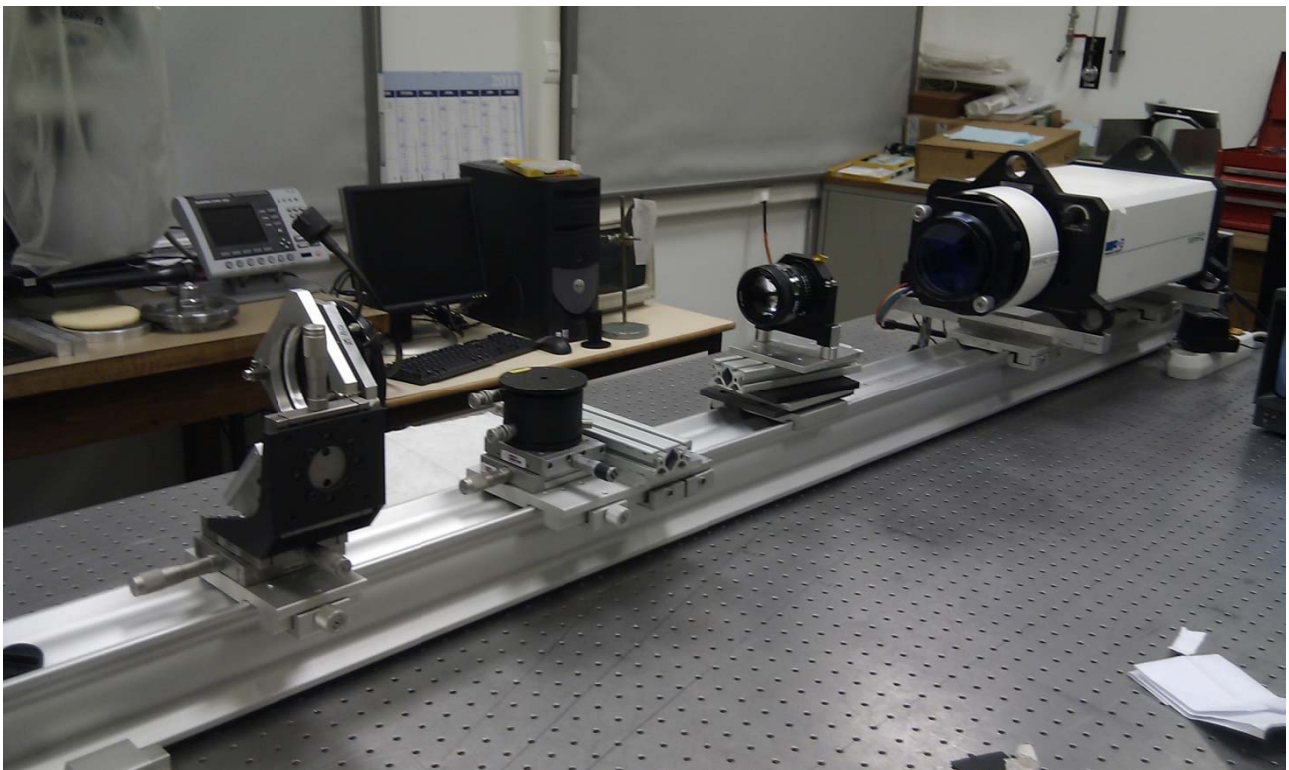


Figure 3 – Picture of the set-up

Data Acquisition Procedure

After the alignment, three sets of data have been recorded:

1. Reference: without the LCFP to get the intrinsic errors of the setup;
2. LCFP turned off: to get the intrinsic errors of the LCFP in its static state;
3. LCFP turned on: different voltages are applied to the LCFP to get the evolution of the WFE as a function of the voltage.

The interferometer is equipped with a HeNe red laser (628nm) while the LCFP has been optimized for the green Fe XIV line (532nm). So the LCFP has not been tested in its optimal configuration.

Due to the previous limits of the used set-up, only 3 voltages have been tested. The selected voltages are referred to the nominal wavelengths of 5312Å, 5325Å and 5338Å. The resultant interferogram is obtained as a resultant of 100 measurements (5x20). In Figure 4 is shown an example of the interferogram obtained with the LCTF.

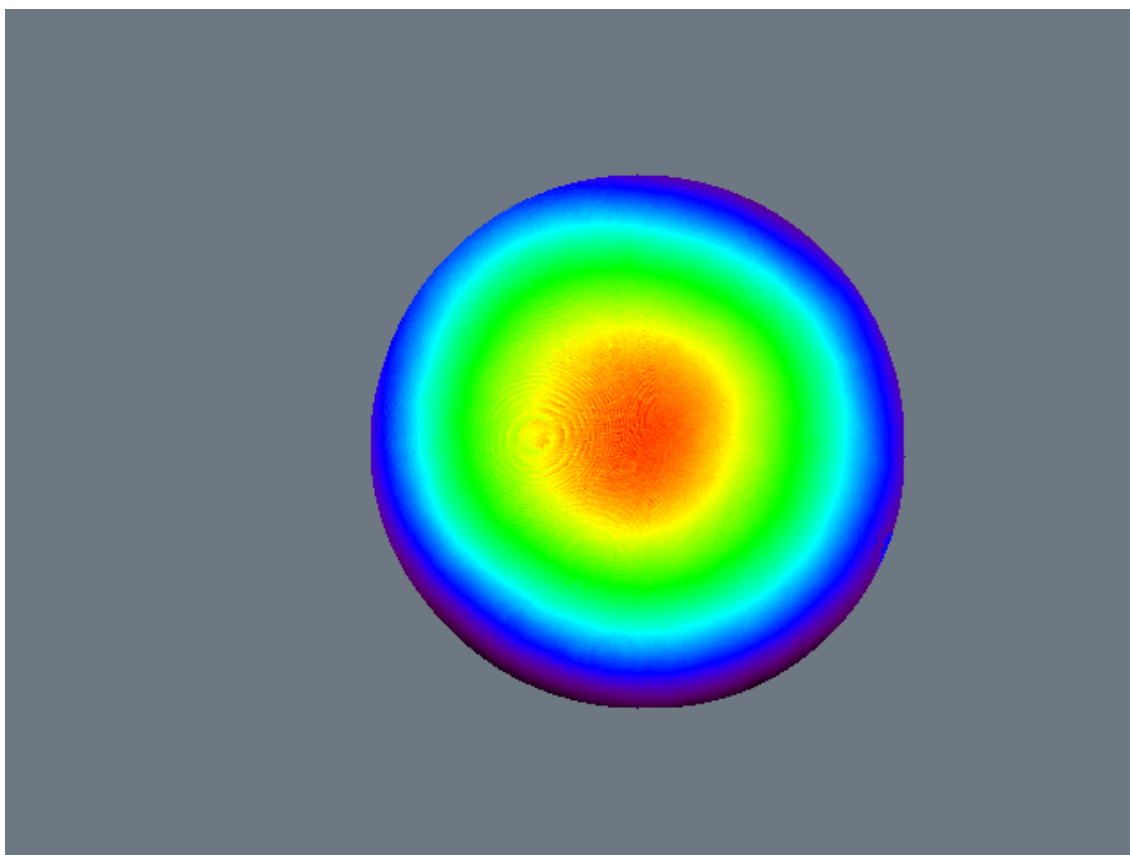


Figure 4 – Interferogram [OPD] of the LCTF

Data Analysis

The data acquired are summarized in Table 2. Note that the LCTF has been tested in a double pass configuration.

	REF	No Voltage 5303,4	5312 nm 5312	5325 nm 5325	5338 nm 5338
Corrected		363,728002	635,680195	159,080244	367,435219
RMS	104,905143	378,554023	644,2782	190,556063	382,117428
X Astig [2]	-53,2578	-32,0181	-107,2551	-91,0093	-29,0473
Y Astig [2]	-27,631	209,9333	139,0206	116,2725	209,7356
X Coma [2]	5,3915	-34,3513	-148,4347	-25,2498	-34,3201
Y Coma [2]	-46,6077	-95,4517	-137,0713	-75,8811	-93,949
Spherical [2]	-15,1118	-4,1084	192,4517	30,3539	-3,2263
X Trefoil [3]	-19,4282	17,821	27,8371	37,4315	18,3962
Y Trefoil [3]	-10,1794	-83,4506	23,4266	31,4596	-87,9867
X Astig [3]	16,2788	-53,037	41,6959	-16,4276	-50,8485
Y Astig [3]	-18,4204	6,7277	-73,8184	-2,5	5,3489
X Coma [3]	-0,1491	122,9267	169,559	13,4766	121,0788
Y Coma [3]	-12,022	41,6946	146,8541	9,9056	43,0083
Spherical [3]	17,9827	-79,0106	-214,9929	-13,7928	-77,9834
X Tetrafoil [4]	8,7911	-12,9015	46,2803	44,2853	-16,3067
Y Tetrafoil [4]	-18,3088	79,3081	-20,013	-18,4386	91,408
X Trefoil [4]	28,1801	72,0875	52,8118	14,2641	68,2233
Y Trefoil [4]	7,0541	9,9662	13,5635	-1,7825	6,2811
X Astig [4]	-16,4669	-72,0103	-89,2638	16,4891	-67,1886
Y Astig [4]	23,567	-59,3783	115,7041	3,41	-57,9166
X Coma [4]	2,7091	84,7188	-114,6641	-0,1694	80,0755
Y Coma [4]	-7,4575	25,9359	-191,7137	-8,9066	27,4626
Spherical [4]	-2,1437	-10,8657	184,608	7,7232	-9,1357
X Pentafoil [5]	-23,6961	89,2536	-16,3471	-17,7894	103,8843
Y Pentafoil [5]	8,0903	-55,7457	-8,3402	-12,8781	-68,7827
X Tetrafoil [5]	4,8323	-70,7151	-41,8508	-19,8549	-68,404
Y Tetrafoil [5]	-17,367	-25,1599	32,4387	4,8716	-18,2993
X Trefoil [5]	-5,4931	38,8272	-70,8919	-5,0359	36,347
Y Trefoil [5]	11,8614	69,5891	-32,5835	1,1009	65,8284
X Astig [5]	-1,8023	-32,2132	135,2937	-8,1309	-27,4837
Y Astig [5]	-5,1594	-36,1532	-105,4911	-0,8858	-37,9362
X Coma [5]	-6,4237	-17,3521	38,2038	-2,757	-21,5995
Y Coma [5]	5,9478	11,365	189,4102	10,9782	15,2444
Spherical [5]	-6,5127	20,0538	-120,44	-1,9158	19,0348

Table 2 – Data Acquired. The values are in nm.

The first column shows the name of the optical aberrations and in the square bracket the order of the corresponding Zernike polynomial. The variation of the 2nd order aberrations vs. the nominal wavelength of the LCTF is in Figure 5. The dominant aberration is the spherical one.

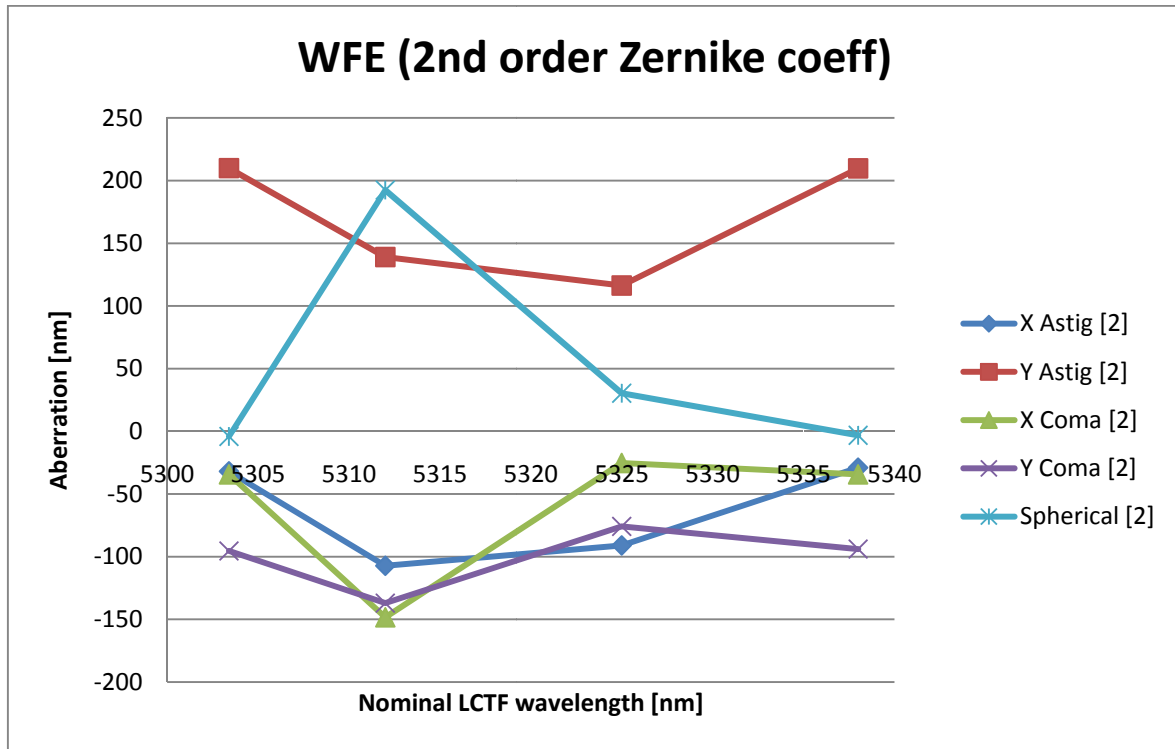


Figure 5 – Variations of the 2nd order Zernike parameters

The resultant imaging quality is shown in Figure 6. The variations are of order of $\frac{1}{4} \lambda$. With the controller turned off, the imaging quality is $\lambda/2$, as expected .

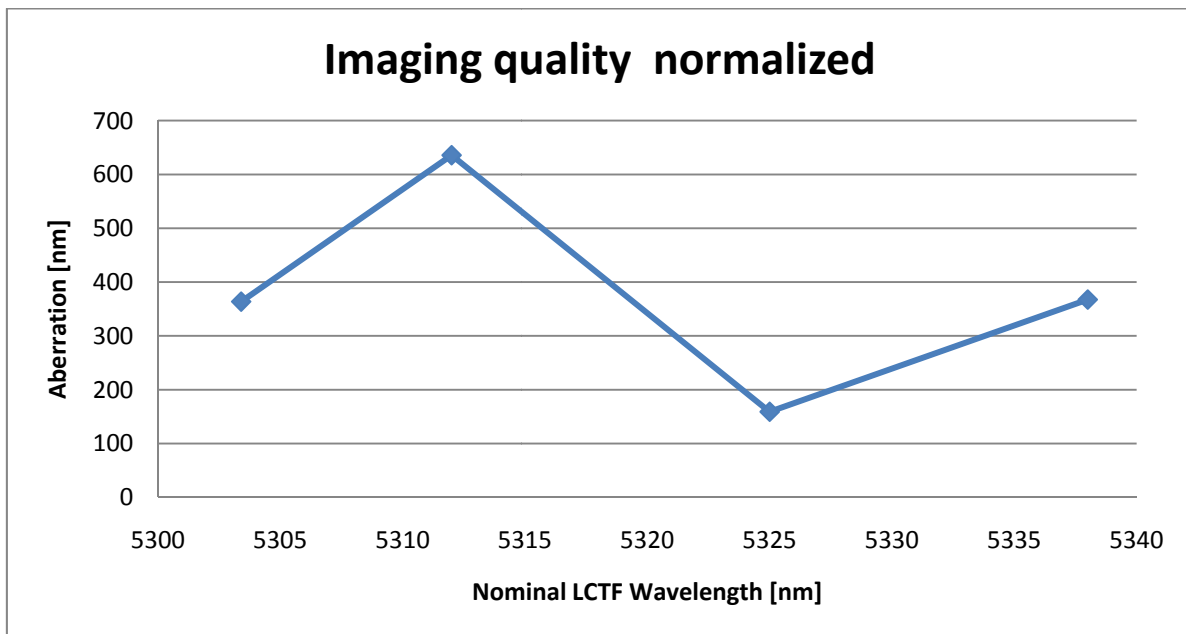


Figure 6 – Imaging quality normalized to the set-up aberrations



LCTF Wavefront error characterization



OATo TR 152
Rev. 0.1
2011.07.25

8

Conclusions

This test shows that the most relevant contribution to the imaging quality of the LCTF is the spherical aberration. The variations of the wave front error are of order of $\frac{3}{4} \lambda$. The non-uniformity of this parameter suggest us a more accurate calibration. However, accurate repeatability tests have to be performed to confirmed the possibility to calibrate the LCTF.

The contributions of the pre-filter and of the LCPR are not taken into account in this analysis.

Further investigations are suggested to confirm the large variation of the WFE while tuning and to evaluate the possibility to calibrate the LCTF.